Study on the efficient removal of azo dyes by heterogeneous photo-Fenton process with 3D flower-like layered double hydroxide

Siqi Bao, Yuqi Shi, Youshan Zhang, Longjie He, Wangyang Yu, Zexiang Chen, Yunfeng Wu and Leijiao Li

ABSTRACT

As organic dyes are the main pollutants in water pollution, seeking effective removal solutions is urgent for humans and the environment. A novel environmentally friendly three-dimensional CoFe-LDHs (3D CoFe-LDHs) catalyst was synthesized by one-step hydrothermal method. Scanning electron microscopy, energy dispersive spectroscopy, Fourier transform infrared spectra, X-ray diffraction, X-ray photoelectron spectroscopy, Brunauer-Emmett-Teller technique as well as UV-Vis diffuse reflectance spectra were used to characterize the prepared samples. The experimental results revealed that 3D CoFe-LDHs exhibited a rapid decolorization of methyl orange and Rhodamine B by heterogeneous photo-Fenton process after reaching the adsorption equilibrium, and the final decolorization efficiency reached 91.18% and 93.56%, respectively. On the contrary, the decolorizing effect of 3D CoFe-LDHs on neutral blue was relatively weak. The initial concentrations of azo dyes, pH and H_2O_2 concentration affected the decolorization of dyes and the catalyst maintained excellent reusability and stability after reuse over five cycles. The quenching experiments found that •OH, $\bullet O_2^-$ and h^+ were the main active substances and reaction mechanisms were further proposed. The study suggests that the synergistic effect of photocatalysis and Fenton oxidation process significantly improved the removal of azo dyes and the synthesized catalyst had potentially promising applications for difficult-to-biodegrade organic pollutants in wastewater.

Key words | active substances, azo dyes, heterogeneous photo-Fenton, layered double hydroxides

Siqi Bao (corresponding author)
Yuqi Shi
Youshan Zhang
Longjie He
Wangyang Yu
Zexiang Chen
Yunfeng Wu
Leijiao Li
School of Chemistry and Environmental Engineering,
Changchun University of Science and Technology,
Changchun 130022,
China;
Jilin Provincial Science and Technology Innovation Center of Optical Materials, and Chemistry,
Changchun 130022,
China;
and
Joint Sino-Russian Laboratory of Optical Materials and Chemistry,
Changchun 130022,
China
E-mail: *baosiqi@cust.edu.cn*

HIGHLIGHTS

- 3D CoFe-LDHs was fabricated and used in efficient removal of organic dyes by photo-Fenton process; the decolorization of MO is highly pH and H_2O_2 dependent.
- Possible reaction mechanism and the stability of 3D CoFe-LDHs were investigated.
- OH, $\bullet O_2^-$ and h^+ formed during photo-Fenton reaction are effective to enhance the decolorization of MO.

doi: 10.2166/wst.2020.293

GRAPHICAL ABSTRACT

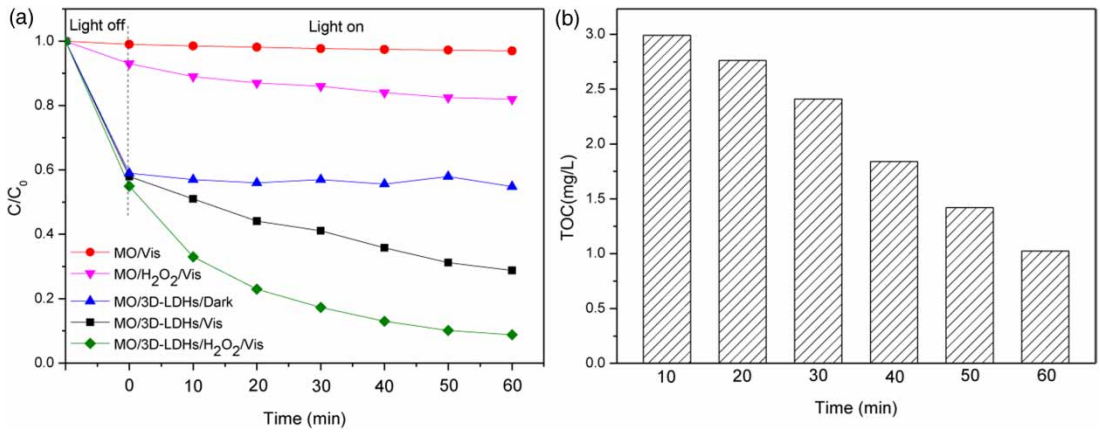

INTRODUCTION

With the rapid development of industrialization and urbanization, environmental problems have gradually attracted great public attention, and water pollution is the typical one. It is well known that the textile printing and dyeing industry relies heavily on organic dyes. If these toxic dyes are directly discharged without treatment, it will greatly harm the natural water environment. Especially, azo dyes and their degradation products are carcinogenic, teratogenic and mutagenic even at extremely low concentrations, which poses a huge threat to human health and ecosystems (Govindan *et al.* 2019; Sarma *et al.* 2019). However, the common methods for removing azo dyes, which include coagulation (Luo *et al.* 2019), adsorption (Guo *et al.* 2019), biodegradation (Liu *et al.* 2019) and membrane separation (Lin *et al.* 2015), are not complete solutions due to the complex molecular structure and biological resistance of azo dyes. Therefore, how to deal with the effluents containing dyes is looming ahead.

Fenton oxidation process is one of the most widely used methods of advanced oxidation processes (AOPs), the advantage of which is that strong oxidizing free radicals (•OH) are generated and used to treat pollutants in water and soil (Dos Santos *et al.* 2020). Nevertheless, the activity of the Fenton oxidation process is affected by the strict pH range, low Fe^{2+} regeneration and excessive ferric sludge. Based on the above, the heterogeneous photo-Fenton procedure occurred as an alternative method for its advantages of wider pH range, less iron-containing sludge and higher oxidation efficiency than the homogeneous photo-Fenton procedure (Dos Santos *et al.* 2020; Goncalves *et al.* 2020). In addition, heterogeneous photo-Fenton catalysts not only retain the advantages of traditional photo-Fenton catalysts, such as being cheap, non-toxic, and easy to separate, but also make up for the shortcomings of having few active sites, poor reusability, low catalytic efficiency and low mineralization efficiency.

In recent years, types of heterogeneous photo-Fenton catalysts have been used to remove various pollutants in water, such as CdS, FeS_2, MnOx, MOFs, TiO_2 and layered double hydroxides (LDHs) (Espinoza *et al.* 2016; Zhao *et al.* 2017; Xu *et al.* 2020). Among them, LDHs have increasingly been focused on as catalytic materials, separation and adsorption materials and biomedical materials due to their large specific surface area, high ion exchange capacity, excellent thermal stability, low preparation cost and environmental friendliness (Zong *et al.* 2018). Yet, the limited active sites of conventional LDHs powders/nanopowders make it difficult to mineralize difficult-to-biodegrade organic pollutants. Nowadays, owing to their higher specific surface area for adsorption, more abundant active sites for pollutant reaction, and a fractal architecture that facilitates an outstanding ability to trap incident light at any angle, three-dimensional LDHs (3D-LDHs) are considered to be ideal heterogeneous photo-Fenton catalysts. Zhang *et al.* (2019) reported 3D MgAl-LDHs showed excellent adsorption performance for Methyl Orange (MO) and Rhodamine B (RhB), and the removal mechanisms were surface adsorption and anion exchange. Xue *et al.* (2018) synthesized 3D NiAl-LDHs/porous anodic aluminum oxide templates that exhibited excellent decolorization of

MO. Dai *et al.* (2019) investigated 3D ZnFe-LDHs composite sponge that exhibited high adsorption ability for As(V) and the maximum adsorption capacity reached 85.7 $mg \cdot g^{-1}$. Wang *et al.* (2018) built a Fenton system containing H_2O_2 and CuNiFe-LDHs to effectively mineralize phenol. However, a high Fe content will destroy the stable hydrotalcite structure and lead to the formation of magnetite particles (Ma *et al.* 2016). Hence, it is necessary to determine the content of Fe in LDHs. To the best of our knowledge, papers about the decolorization of azo dyes by individual 3D-LDHs without templates are rare.

Herein, the aims of the work are: (1) to synthesize an example of flower-like 3D CoFe-LDHs catalyst via a simple one-step hydrothermal method; (2) to characterize the morphological features, structures and physical and chemical properties of the as-prepared catalyst by SEM, XRD, FT-IR, XPS, BET and UV-Vis DRS; (3) to investigate the decolorization of MO, RhB and neutral blue, the influencing factors of decolorization and reaction mechanisms under the synergistic effect of photocatalytic and Fenton oxidation process. The results can lay a theoretical foundation for the practical application of 3D-LDHs in the field of difficult-to-biodegrade organic wastewater.

MATERIAL AND METHODS

Chemicals and materials

$Co(NO_3)_2 \cdot 6H_2O$, $Fe(NO_3)_3 \cdot 9H_2O$, NH_4F, urea, and anhydrous methanol (≥99.5%) were of analytical grade and purchased from Shanghai Macklin Biochemical Co., Ltd. The azo dyes MO (≥85%), RhB (96%) and neutral blue (≥82%) were analytical reagents and purchased from Sinopharm Chemical Reagent Co., Ltd. All reagents were used directly without further purification.

Preparation of 3D CoFe-LDHs

3D CoFe-LDHs were synthesized via a hydrothermal method according to literature reported by Gao *et al.* (2019). In a typical synthesis, $Co(NO_3)_2 \cdot 6H_2O$ (2.619 g) and $Fe(NO_3)_3 \cdot 9H_2O$ (1.212 g) were dissolved in methanol anhydrous (30 mL) to form a clear salt solution with Co^{2+}/Fe^{3+} molar ratio of 2.0. Then, urea (1.261 g) and NH_4F (0.1 g) were immediately added into the salt solution and vigorously stirred for 2 h. Afterward, the solution was transferred to a 100 mL Teflon-lined stainless-steel autoclave. The autoclave was sealed and kept at 120 °C for 12 h. A brown solid precipitate was collected by centrifugation and washed with distilled water and ethanol several times. Finally, the product was dried in a vacuum oven at 70 °C overnight.

Characterization

Combined with a variety of characterization methods, the surface morphology, structure, and physical and chemical properties of 3D CoFe-LDHs were investigated. The crystallographic structure of the catalyst was measured by power X-ray diffractometer with the diffraction angle range from 5° to 70° (XRD). The morphology and structure of the composite was studied by scanning electron microscopy (SEM, JSM-6510). The material composition and functional groups were examined by recording the Fourier transform infrared spectra (FT-IR, IFS 66 V/S, Germany). The elemental analysis was analyzed by energy dispersive spectroscopy (EDS) attached to SEM. X-ray photoelectron spectroscopy (XPS) results of catalysts were determined through a Rigaku 2500/PC spectrometer. The Brunauer-Emmett-Teller (BET) surface area of catalysts was determined on a Micromeritics Tristar II3020 apparatus. The decolorization experiments of azo dyes were observed using an Ultraviolet-visible (UV-Vis) spectrophotometer (UVmini-1240, SHIMADZU). UV-Vis diffuse reflectance spectra (UV-Vis DRS) of the catalyst was obtained on a U-4100 UV-Vis spectrophotometer. Total organic carbon of the dye was analyzed using a TOC analyzer (AA-6000CF).

Experiments procedure

The experiments of azo dyes decolorization were performed using a self-made photoreaction device. The light source was an 80 W xenon lamp (without filter) used to simulate sunlight, the spectral distribution is found in Figure S1 (supplementary information). The light intensity was 5000 Lex and the distance between the xenon lamp and samples was 15 cm under the experimental conditions. 3D CoFe-LDHs (20 mg) was added into azo dyes solutions (40 mL). The reaction solution was kept on the magnetic stirrer during the reaction. Before irradiation, the solution was stirred in the dark for 30 min to obtain the adsorption-desorption equilibrium. Then the suspension was exposed under the simulated sunlight while being magnetically stirred. Samples from reaction systems were withdrawn at regular intervals and filtered with a water filter before measurement. The MO, RhB and neutral blue samples were analyzed by recording the largest absorption peak at

464, 554 and 590 nm, respectively, for analysis subjected to UV-Vis spectroscopic measurements. Dye decolorizations were calculated according to the following equation:

$$\text{Dye decolorization} = \left(\frac{C_0 - C_t}{C_0}\right) \times 100\% \quad (1)$$

where C_0 is the initial concentration of dye, and C_t is the dye concentration at the corresponding reaction time.

RESULTS AND DISCUSSION

Catalyst characterization

The morphology, structure and elemental constitution of 3D CoFe-LDH are shown in Figure 1. X-ray diffraction data (Figure 1(a)) manifest that the reflection peaks in the pattern for the catalyst at $2\theta = 11.05°$, $22.44°$, $33.11°$, $33.88°$, $38.16°$, $45.44°$, $59.05°$ and $60.68°$ correspond to planes of (003), (006), (101), (012), (015), (018), (110) and (113) respectively, suggesting a highly crystalline structure and a high purity of the LDH phase, which is consistent with a previous report (Arif *et al.* 2019). Figure 1(b) shows that we successfully synthesized a flower-like microporous sample. These microspheres are assembled into a discrete layer structure from many irregularly and randomly arranged nanosheets. Also, there are a large number of interconnected macroporous networks between layers and hierarchies. On the one hand, the flower-like structure provides more reactive sites, which is expected to increase the adsorption capacity of the catalyst and significantly enhance the removal of pollutants (Sanchez *et al.* 2005). On the other hand, combined with the biomimetic and bioinspired thinking, the flower-like structure makes full use of solar energy through multiple internal reflections and improves the light-trapping capability of the catalyst (Serrà *et al.* 2019). In Figure 1(c), the catalyst sample shows a typically broad band at around 3,424 cm^{-1} corresponding to interlayer water molecules where hydrogen is bonded to the metal-OH group (Ma *et al.* 2016). The band at about 1,631 cm^{-1} corresponds to the bending mode of water molecules. The characteristic bands at around 673 and 492 cm^{-1} in the low wavenumber region relate to the brucite-like structure and can be attributed to metal-OH bending and metal-O stretching vibrations in the octahedral hydroxyl sheets, respectively (Cheng *et al.* 2014). The typical absorption peaks of carbonate ions are approximately 1,380 cm^{-1}. In the meantime, two weak bands at 2,850 and 2,920 cm^{-1} can be ascribed to the stretching vibration of C-H (Xia *et al.* 2015), indicating that a little methanol is still remaining in the product. These assignments are in common with previously reported results

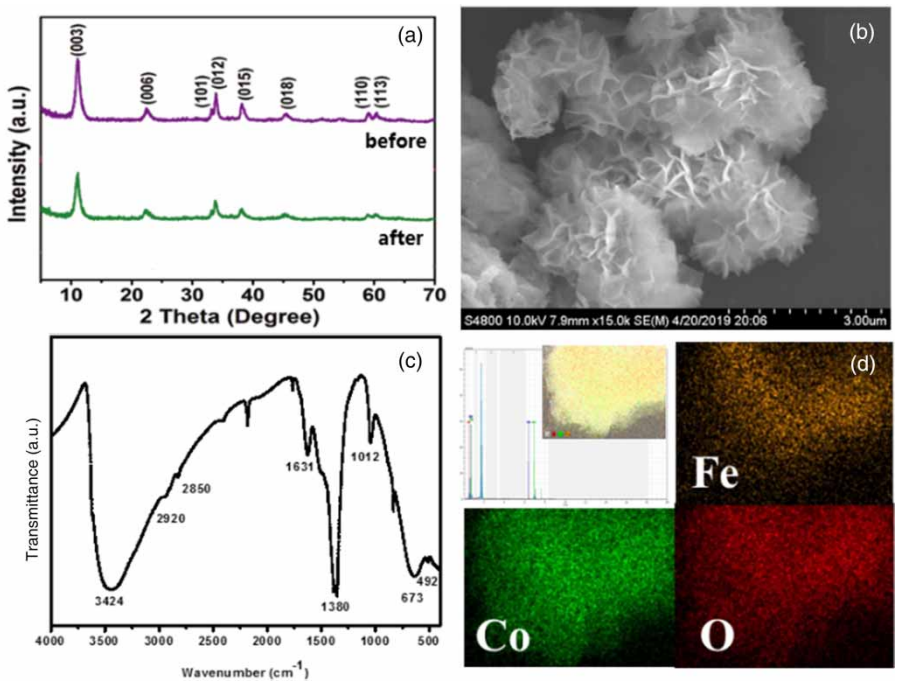

Figure 1 | Structural characterizations of 3D CoFe-LDHs. (a) XRD pattern, (b) SEM image (c) FT-IR and (d) EDS mapping.

(Yang *et al.* 2019). A typical EDS spectrum of catalyst in Figure 1(d) obviously proved the overlapping of corresponding elements of Co, Fe and O, authenticating the uniform dispersion of 3D CoFe-LDHs. In order to further confirm the surface electronic state and elemental composition of the catalyst, XPS test were performed. Figure 2(a) displays that the survey XPS spectrum contains Co, Fe, O and C, which is consistent with EDS mapping. For the Co 2p spectrum in Figure 2(b), the peaks located at 783.9/801.3 eV and 782.1/798.0 eV can be asssigned to the main peaks of Co^{2+} ($2p_{3/2}/2p_{1/2}$) and Co^{3+} ($2p_{3/2}/2p_{1/2}$), accompanied by the satellite peaks of Co and Co^{2+} salt at 787.4/804.0 eV (Zhao *et al.* 2020). The Fe 2p spectrum (Figure 2(c)) features multiple remarkable peaks at 711.9/723.3 eV, 714.5/727.0 eV and 719.2 eV, corresponding to $2p_{3/2}$ and $2p_{1/2}$ orbits of Fe^{2+} and Fe^{3+} as well as Fe Sat. orbits, respectively (Hao *et al.* 2019). The BET surface area of the catalyst is observed in Figure S2 (supplementary information). The large BET surface area (103.7 $m^2 \cdot g^{-1}$) provides more reaction sites for the catalyst to remove polluntants. Moreover, the UV-vis DRS spectra of the catalyst was analyzed by a UV-vis spectrophotometer with a wavelength range of 200–800 nm (Figure S3). It can be seen that the prepared catalyst had strong absorption in the ultraviolet region and the visible region, and the absorption range was wide, indicating that the catalyst is expected to be used as a heterogeneous photo-Fenton catalyst.

Decolorization of azo dyes under different systems

MO (anionic dye), RhB (cationic dye) and neutral blue (neutral dye) were selected as the target pollutants to evaluate the removal effect of 3D CoFe-LDHs on organic pollutants. Figure S4 reveals 3D CoFe-LDHs showed stronger decolorization of MO and RhB than neutral blue. This is probably because the prepared catalyst is composed of positively charged metal cations and negatively charged anions between the layers. Thus, the electrostatic interaction between the charge on the surface of the adsorbent and the molecular structure of the cationic dye/anionic dye is stronger than that of the neutral dye, resulting in the

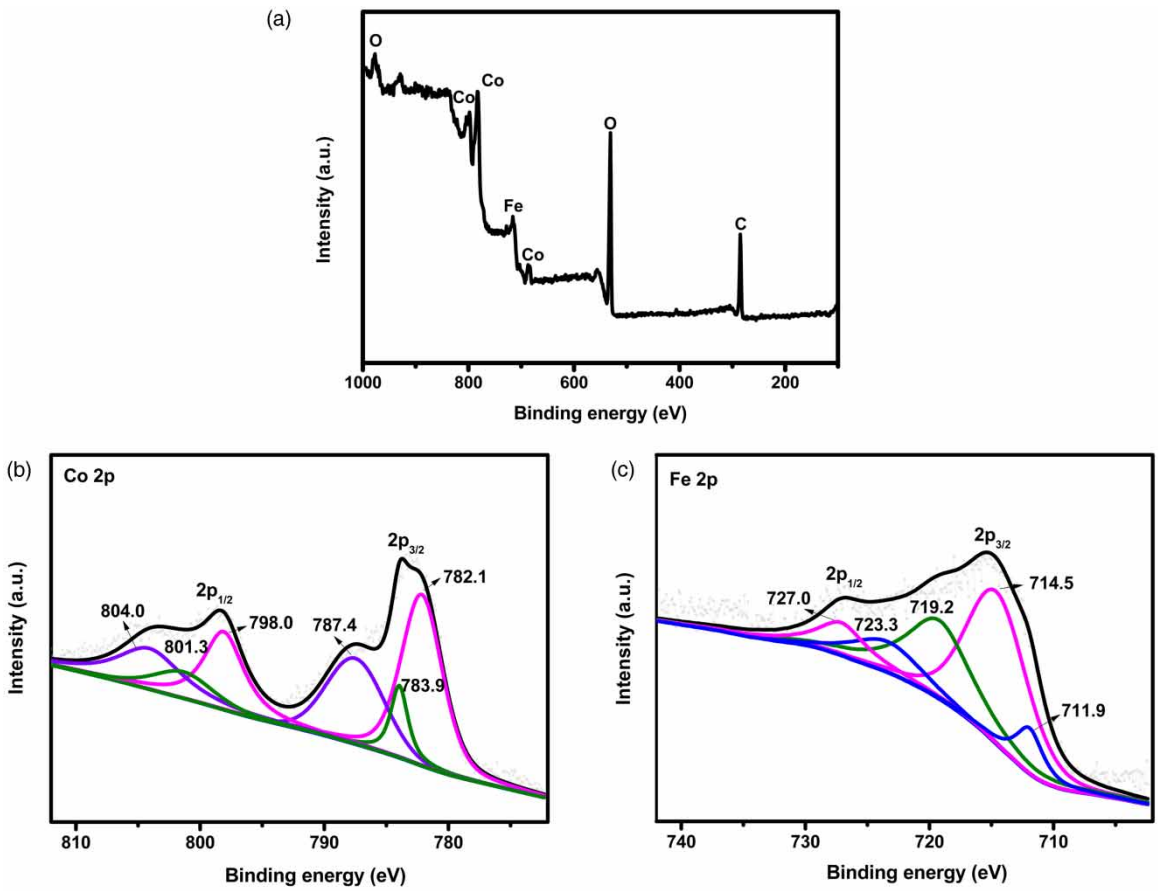

Figure 2 | XPS of 3D CoFe-LDHs (a) survey scan, (b) cobalt 2p and (c) iron 2p.

adsorption effect of 3D CoFe-LDHs on MO and RhB being much better than that of neutral blue. Moreover, RhB has photosensitivity under the simulated sunlight, and the photo-stability of MO is higher than RhB, so the decolorization of RhB is higher than that of MO.

Control experiments were conducted to deeply investigate the decolorization of azo dyes under different systems. The experimental results are shown in Figure 3.

As shown from Figure 3(a), there is no significant concentration change of MO under simulated sunlight, indicating that MO is resistant to simulated sunlight. The decolorization of MO was 18.05% within 60 minutes after H_2O_2 was added. When applied with 3D CoFe-LDHs alone, the adsorption equilibrium was achieved at 30 minutes and the decolorization efficiency reached 42.3% owing to the large specific surface area of the catalyst. A much higher efficiency of MO (72.2%) was observed under simulated sunlight, which is attributed to electronic transition of the catalyst under light excitation, thereby simultaneously generating positive holes (h^+) in the valence band (VB) and photo-induced negative electrons (e^-) in the conduction band (CB) (Equation (2)). Then h^+ could react with H_2O or OH^- in the system to generate ·OH with strong oxidation ability (Equations (3) and (4)). And the superoxide radicals ($\cdot O_2^-$) could be generated via the reaction between the electrons and oxygen on the surface of the catalyst (Equation (5)). Unfortunately, it is difficult to use h^+ and e^- effectively due to the rapid recombination of photo-generated electron-hole pairs, thus the decolorization efficiency was not ideal. In order to further promote the decolorization of MO, a simple and important strategy is the addition of H_2O_2 to the reaction. A significant improvement in decolorization efficiency was obtained after adding H_2O_2, more than 91%. Under this reaction condition, it is a typical heterogeneous photo-Fenton process, in which H_2O_2 as a strong trapping agent of e^- in the CB could effectively reduce the chance of recombination of photo-generated electrons and holes and generate a large amount of ·OH to promote the activity of the catalyst (Equations (6) and (7)) (Cai *et al.* 2016). Simultaneously, Fe^{3+} in the system can also generate ·OH under simulated sunlight (Equation (8)) (Dos Santos *et al.* 2020). In addition, Fe^{3+} can react with electrons to form Fe^{2+} (Equation (9)), maintaining the continuation of Equation (6).

$$3D\ CoFe\text{-}LDHs + h\vartheta \rightarrow 3D\ CoFe\text{-}LDHs\ (h^+ + e^-) \quad (2)$$

$$h^+ + H_2O \rightarrow H^+ + \cdot OH \quad (3)$$

$$h^+ + OH^- \rightarrow \bullet OH \quad (4)$$

$$O_2 + e^- \rightarrow \bullet O_2^- \quad (5)$$

$$H_2O_2 + Fe^{2+} \rightarrow Fe^{3+} + OH^- + \bullet OH \quad (6)$$

$$H_2O_2 + e^- \rightarrow \bullet OH + OH^- \quad (7)$$

$$Fe^{3+} + H_2O + h\vartheta \rightarrow \bullet OH + Fe^{2+} + H^+ \quad (8)$$

$$Fe^{3+} + e^- \rightarrow Fe^{2+} \quad (9)$$

Furthermore, an obvious change in total organic content (TOC) of MO was observed during the heterogeneous photo-Fenton process. Figure 3(b) displays that the 3D CoFe-LDHs had a high mineralization degree of MO. It was also found that the decolorization of MO

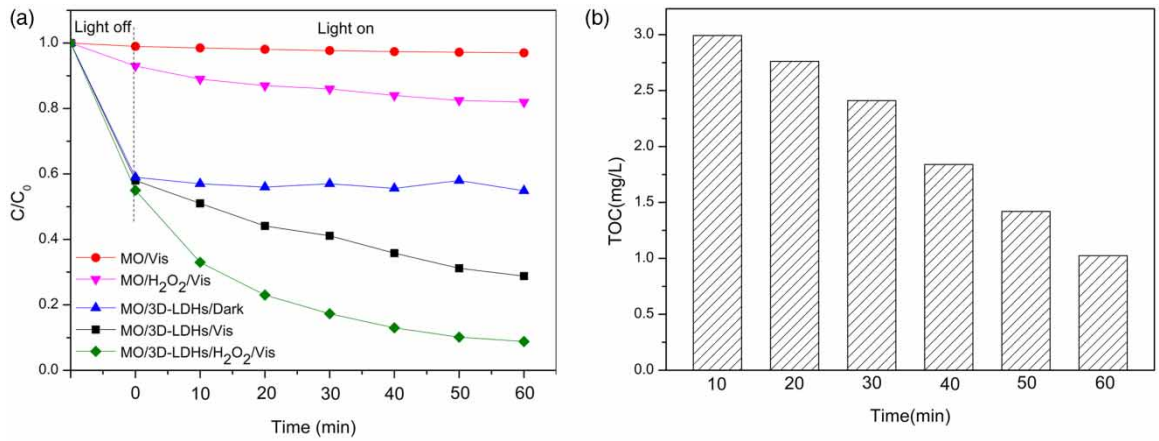

Figure 3 | (a) Control experiments for the decolorization of MO, (b) TOC removal of MO by heterogeneous photo-Fenton process ([MO] = 5 mg/L, 3D-LDHs dosage = 20 mg, pH = 3.2 and $[H_2O_2]$ = 1.44 mM).

was always faster than the mineralization. For example, the corresponding TOC value decreased from 2.992 to 1.024 mg/L and reached about 65.78% after an hour, whereas the decolorization of MO was 91.18% at the same time. In summary, the synergistic effect of photocatalytic and Fenton oxidation processes significantly improves the decolorization and mineralization of MO, which is in good agreement with the results reported previously (Wang *et al.* 2020).

To further study the decolorization of azo dyes in the real water environment, two kinds of actual wastewater were collected from Sichuan FAW Toyota Motor Co., Ltd, which respectively corresponded to degreasing wastewater and electrophoretic wastewater. The quality parameters of the two kinds of wastewater and the decolorization behavior of the MO in them are shown in Table S1 and Figure S5, respectively. The results suggest that the decolorization of MO in electrophoretic wastewater was significantly higher than that of degreasing wastewater under simulated sunlight, and the specific decolorization efficiency reached 83.53% and 27.2%, respectively. The reason for this phenomenon may be that the higher pH of the degreasing wastewater is not conducive to the reaction, so the decolorization efficiency is weaker than that of electrophoretic wastewater. In addition, the chemical oxygen demand (COD) of electrophoretic wastewater is higher than that of degreasing wastewater, and the COD is larger; the pollution of water bodies by organic compounds is more serious. Under the synergy of various organic and inorganic substances, the decolorization of MO in electrophoretic wastewater was better.

Effect of reaction conditions on the removal of MO

Effect of MO concentrations

Three concentrations (2, 5 and 10 mg/L) of MO were selected to investigate the effect of different initial concentrations of MO on their decolorization.

As shown in Figure 4, the study found that as the initial concentration of MO increased from 2 to 5 mg/L, the removal rate increased from 84.12% to 91.18%. This is because with the concentration of MO augmenting, the corresponding MO content adsorbed on the surface of the catalyst increased, promoting the decolorization. Nevertheless, when the concentration of MO continued to increase to 10 mg/L, the decolorization efficiency decreased. It might be because intermediate products generated during the reaction would gradually accumulate on the surface of the catalyst, covering the active sites of the catalyst, ultimately leading to a slight decrease in the decolorization. The results are similar to previously reported results (Chen *et al.* 2017).

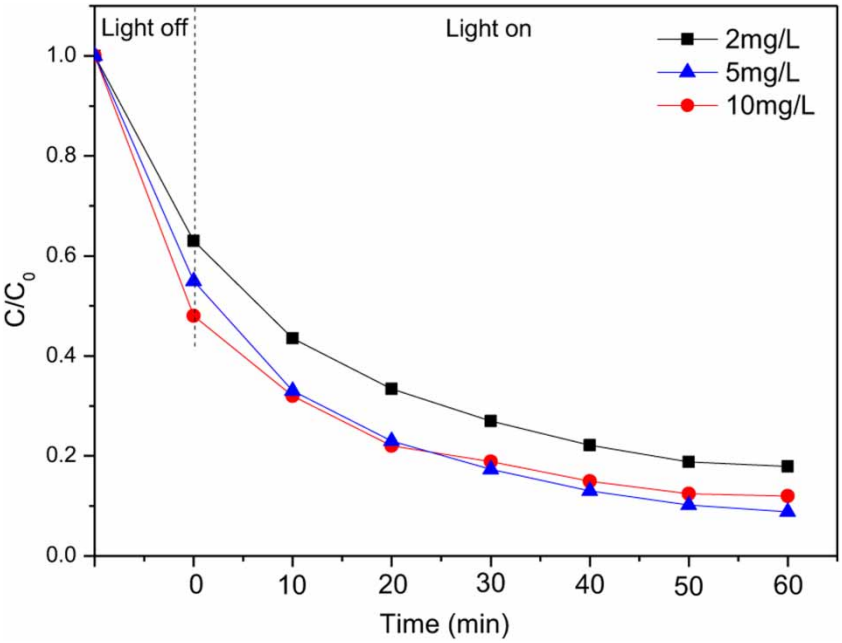

Figure 4 | Effect of different MO concentrations on the decolorization of MO (3D-LDHs dosage = 20 mg, pH = 3.2 and $[H_2O_2]$ = 1.44 mM).

Effect of initial pH

It is well known that the pH value of the solution has a greater impact on the heterogeneous photo-Fenton process (Yuan *et al.* 2018). The effect of pH on the decolorization of MO is illustrated in Figure 5. The different pH of the MO solution were adjusted to 2.1, 3.2, 7.2, and 11.7 with H_2SO_4 and NaOH, while other conditions were kept the same with the above experiment.

As shown in Figure 5, the decolorization of MO under acidic conditions is better than in alkaline conditions. When the solution was strongly acidic or alkaline, the high concentration of H^+ or OH^- in the solution would inhibit the excited transition of electrons in 3D CoFe-LDHs into photo-generated electrons, reducing the generation of active radicals. Moreover, the lower decolorization at pH 2.1 than 3.2 was attributed to the excess H^+ ions in the system that eliminated the •OH (Equation (10)), inhibiting the decolorization of MO. The decolorization efficiency at pH 7.2 was higher than that at pH 11.7, which may be because, according to the Nernst equation, the higher the pH value, the higher the valence and conduction band energy level positions are, reducing the oxidizing ability of the holes. These are not conducive to the progress of the heterogeneous photo-Fenton oxidation reaction. The results of this experiment are the same as the study by Bai *et al.* (2017).

$$\bullet OH + H^+ + e^- \rightarrow H_2O \quad (10)$$

Effect of H_2O_2 concentrations

The effect of H_2O_2 dosage on MO degradation was investigated with different concentrations of H_2O_2 under simulated sunlight. The results are presented in Figure 6.

As can be seen from Figure 6, with the addition of H_2O_2 increasing from 1.44 to 2.54 mM, the removal efficiency of MO increased from 91.18% to 96.15%. When the concentration of H_2O_2 continued to increase to 3.61 mM, the removal efficiency of MO did not increase significantly. The reason for this phenomenon may be that H_2O_2 can generate the powerful oxidation agent •OH. With the concentration of H_2O_2 increasing continuously, the amount of •OH generated also continued to grow. However, the little increase subsequently was due to the fact that a higher concentration of H_2O_2 scavenging of •OH would occur (Equations (11) and (12)) (Velo-Gala *et al.* 2017). In other words, H_2O_2 was also a quencher of •OH from a certain perspective, which is consistent with the previous report (Wang

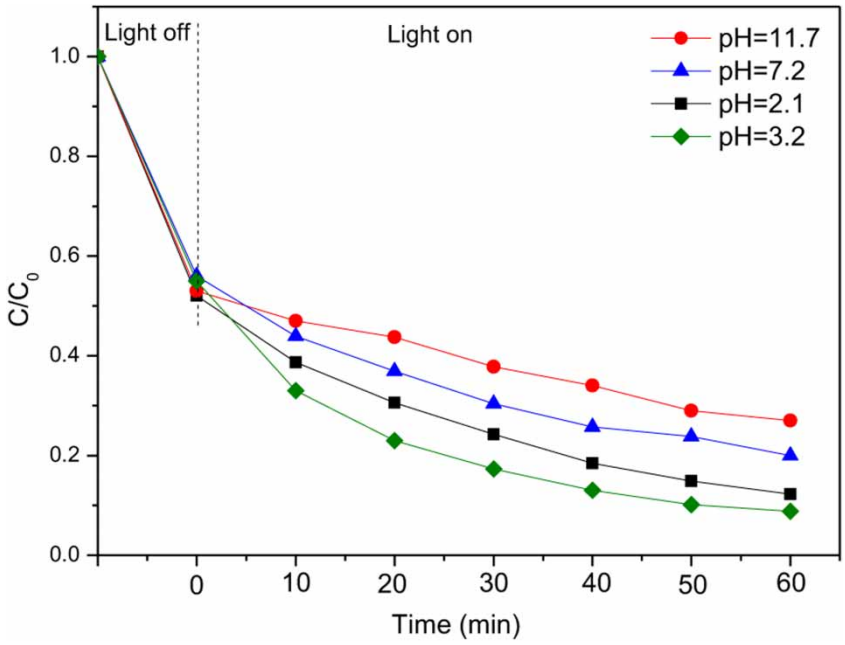

Figure 5 | Effect of different initial pH on the decolorization of MO ([MO] = 5 mg/L, 3D-LDHs dosage = 20 mg and [H_2O_2] = 1.44 mM).

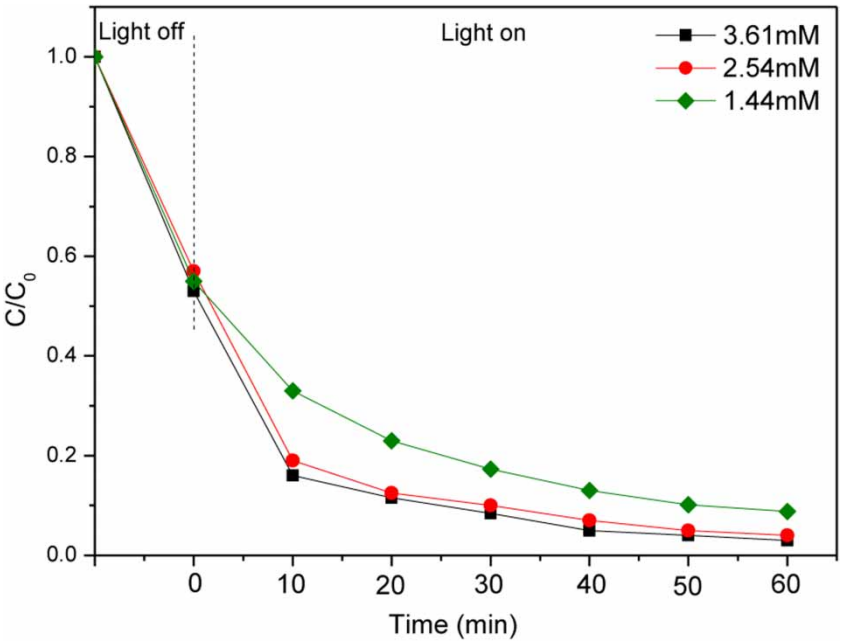

Figure 6 | Effect of different H_2O_2 concentrations on the decolorization of MO ([MO] = 5 mg/L, 3D-LDHs dosage = 20 mg and pH = 3.2).

et al. 2017).

$$\bullet OH + H_2O_2 \rightarrow H_2O + HO_2\bullet \quad (11)$$

$$HO_2\bullet + \bullet OH \rightarrow H_2O + O_2 \quad (12)$$

Recycling of catalyst

Repeated avaliability of the heterogeneous photo-Fenton catalyst is an important property for its application, so recycling reactions were implemented. In each test, the catalyst was collected and reused after washing with water and drying. The situation of cycling for five times under simulated sunlight is shown in Figure 7.

During the experiments, the initial concentrations of MO, H_2O_2 and 3D CoFe-LDHs were 5 mg/L, 2.54 mM and 20 mg respectively. The reaction pH value and time were 3.2 and 60 min. The recycling experiments results revealed that MO degradation during five cycles can still reach more than 75%, indicating that 3D CoFe-LDHs possessed good stability and activity in heterogeneous photo-Fenton process, which is much better than the results reported before (Li *et al.* 2017). Thence, 3D CoFe-LDHs is an excellent candidate to remove azo dyes for its reutilization. Meanwhile, the XRD and XPS spectrums of the samples after five cycles of recycling were determined. It can be seen from Figure 1(a) and Figure S6, there is basically no obvious shift in the position of the peak, but the intensity of the peak has a downward trend. This may indicate that the structure of the catalyst after the reaction hardly changed, showing excellent stability.

Reaction mechanism

Studies have shown that the removal of organic pollutants is mainly because of a series of active substances generated during the reaction process. In order to further explore the decolorization mechanism of MO during heterogeneous photo-Fenton process, quenching experiments of active substances were performed. Isopropyl alcohol (IPA), benzoquinone (BQ), sodium azide (NaN_3), silver nitrate ($AgNO_3$) and ammonium oxalate ($(NH_4)_2C_2O_4$) were added as quenchers for hydroxyl radicals (•OH), superoxide radicals ($\bullet O_2^-$), singlet oxygen ($^1O_2$), electron (e^-) and holes (h^+) respectively (Guan *et al.* 2017). During the experiments, 0.8 mM of IPA, BQ, NaN_3, $AgNO_3$ or $(NH_4)_2C_2O_4$ was added to the system.

In Figure 8, it can be observed that the decolorization efficiency without quencher, IPA, BQ, NaN_3, $AgNO_3$ and $(NH_4)_2C_2O_4$ was 96.15%, 38.49%, 67.28%, 95.36%, 90.53% and 53.88%, respectively. The decolorization of MO was almost not affected by the addition of NaN_3. On the contrary, the decolorization of MO was sharply decreased with the addition of IPA, BQ and $(NH_4)_2C_2O_4$, which indirectly showed that •OH, $\bullet O_2^-$ and h^+ generated

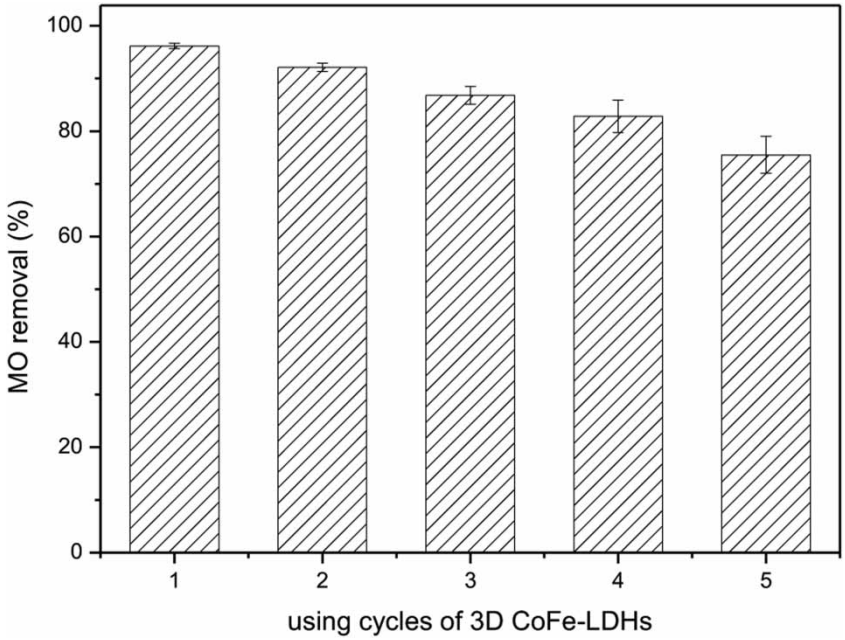

Figure 7 | Recycling experiments of 3D CoFe-LDHs ([MO] = 5 mg/L, 3D-LDHs dosage = 20 mg, pH = 3.2 and $[H_2O_2]$ = 2.54 mM).

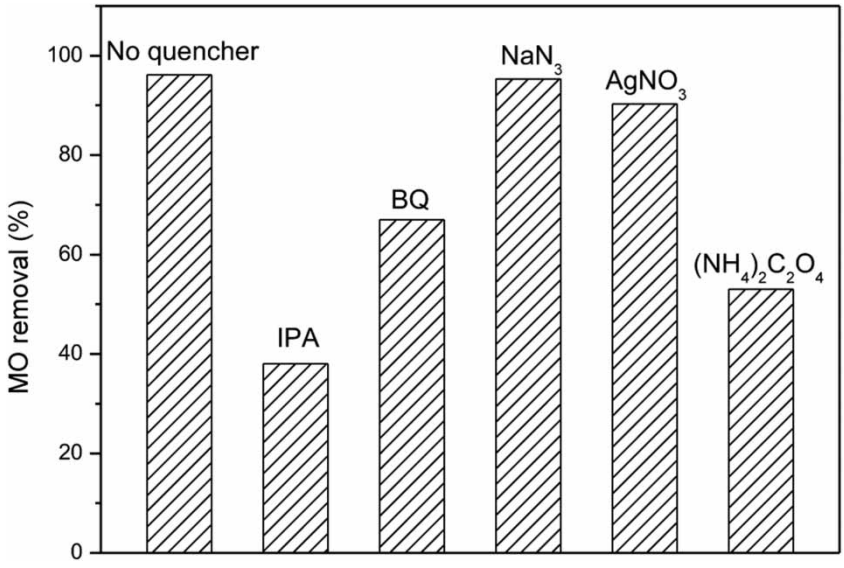

Figure 8 | Quenching experiments of active substances ([MO] = 5 mg/L, 3D-LDHs dosage = 20 mg, pH = 3.2 and $[H_2O_2]$ = 2.54 mM).

during the heterogeneous photo-Fenton process were the main anticipants.

According to the discussion above and previous reports (Dos Santos *et al.* 2019; Serrà *et al.* 2019; Arroyo-Gómez *et al.* 2020), a possible reaction mechanism is proposed and illustrated. At the beginning period of the heterogeneous photo-Fenton process, the flower-like structure of the catalyst provided a large number of adsorption sites, so that part of the MO adsorbed on the catalyst surface. Then, the Fenton oxidation process would occur in the presence of H_2O_2, and the strong oxidizing •OH generated could decolorize MO (Equation (6)). Subsequently, the heterojunction structure of 3D CoFe-LDHs promoted the photo-generated electron-hole pairs to separate, leaving h^+ in the

VB and e^- in the CB under simulated sunlight (Equation (2)). The photo-generated electrons were transformed to oxidizing $\cdot O_2^-$ with O_2 (Equation (5)). The generated $\cdot O_2^-$ one hand could further react with H_2O to produce •OOH and H_2O_2 (Equations (13)–(15)), on the other hand $\cdot O_2^-$ could become another source of •OH (Equations (16) and (17)). Meanwhile, the h^+ combined with OH^- or H_2O, which converted into •OH (Equations (3) and (4)). Besides, the •OH also generated by the direct photolysis of H_2O_2 (Equation (18)) and the capture of H_2O_2 by photo-generated electrons (Equation (7)). These active substances accelerated the decolorization of MO by attacking azo groups, opening the $N=$ N bonds and breaking the long conjugated π bond. Because a large number of •OH were consumed during the reaction process, the new •OH needed to be produced. In this heterogeneous photo-Fenton system, Fe^{2+} could be regenerated via the reaction between Fe^{3+} and H_2O_2/OH^- (Equations (19) and (20)) and Equations (8) and (9), thus sustaining the photo-Fenton reaction. Then more •OH could be produced as more Fe (II) was regenerated to react with H_2O_2.

$$\bullet O_2^- + H_2O \rightarrow \bullet OOH + OH^- \quad (13)$$

$$2 \bullet OOH \rightarrow H_2O_2 + O_2 \quad (14)$$

$$\bullet OOH + H_2O + e^- \rightarrow H_2O_2 + OH^- \quad (15)$$

$$\bullet O_2^- \xrightarrow{h^+} H_2O_2 \xrightarrow{e^-} \bullet OH \quad (16)$$

$$\bullet O_2^- \xrightarrow{e^-} H_2O_2 \xrightarrow{e^-} \bullet OH \quad (17)$$

$$H_2O_2 + \text{visible light} \rightarrow \bullet OH + OH^- \quad (18)$$

$$Fe^{3+} + H_2O_2 \rightarrow Fe^{2+} + HO_2 \bullet + H^+ \quad (19)$$

$$Fe^{3+} + OH^- + h\,\nu \rightarrow Fe^{2+} + \bullet OH \quad (20)$$

CONCLUSION

In this work, a novel flower-like catalyst 3D CoFe-LDHs was synthesized via one-step hydrothermal method. It has been demonstrated that during the initial period of heterogeneous photo-Fenton process, the adsorption effect of 3D CoFe-LDHs on MO and RhB is obvious and about 40–55% of dyes was removed due to its high specific surface area. Then a highly efficient decolorization of MO and RhB under simulated sunlight was shown. Experiments revealed that the decolorization of 3D CoFe-LDHs is more effective for removing MO and RhB than neutral dye, and is highly dependent on pH and concentrations of dyes. The addition of different concentrations of H_2O_2 and different kind of quenchers both proved that •OH, $\cdot O_2^-$ and h^+ are effective to promote the decolorization of dyes under the synergistic effect of photocatalysis and Fenton oxidation process. What is more, the catalyst showed excellent reusability and stability. All in all, the novel 3D CoFe-LDHs is expected to seek to remove difficult-to-biodegrade organic pollutants from wastewater and realize high mineralization under the synergistic effect of photocatalytic and Fenton oxidation process.

ACKNOWLEDGEMENTS

This work was financially supported by Thirteenth Five-Year Program for Science and Technology of Education Department of Jilin Province (JJKH20200803KJ), the Youth Fund of Changchun University of Science and Technology (XQNJJ-2019-14), Natural Science Foundation Project of Jilin Province (20200201082JC).

SUPPLEMENTARY MATERIAL

The Supplementary Material for this paper is available online at https://dx.doi.org/10.2166/wst.2020.293.

REFERENCES

Arif, M., Yasin, G., Shakeel, M., Mushtaq, M. A., Ye, W., Fang, X. Y., Ji, S. F. & Yan, D. P. 2019 Hierarchical CoFe-layered double hydroxide and g-C_3N_4 heterostructures with enhanced bifunctional photo/electrocatalytic activity towards overall water splitting. *Mater Chem Front.* **3**, 520–531.

Arroyo-Gómez, J. J., Toncón-Leal, C. F., dos Santos, A. J., Moreno, M. S., Sapag, K. & Martínez-Huitle, C. A. 2020 Fe/SBA-15: characterization and its application to a heterogeneous solar photo-Fenton process in order to decolorize and mineralize an azo dye. *Mater. Lett.: X.* **5**, 100034.

Bai, J. F., Liu, Y., Yin, X. H., Duan, H. T. & Ma, J. H. 2017 Efficient removal of nitrobenzene by Fenton-like process with Co-Fe layered double hydroxide. *Appl. Surf. Sci.* **416**, 45–50.

Cai, C., Zhang, Z., Liu, J., Shan, N., Zhang, H. & Dionysiou, D. D. 2016 Visible light-assisted heterogeneous Fenton with $ZnFe_2O_4$ for the degradation of Orange II in water. *Appl. Catal. B: Environm.* **182**, 456–468.

Chen, J. B., Wang, Y., Qian, Y. J. & Huang, T. Y. 2017 Fe(III)-promoted transformation of β-lactam antibiotics: hydrolysis vs oxidation. *J. Hazard. Mater.* **335**, 117–124.

Cheng, J. P., Liu, L., Zhang, J., Liu, F. & Zhang, X. B. 2014 Influences of anion exchange and phase transformation on the supercapacitive properties of α-$Co(OH)_2$. *J. Electroanal. Chem.* **722–723**, 23–31.

Dai, X. H., Zhang, S. X., Waterhouse, G. I. N., Fan, H. & Ai, S. Y. 2019 Recyclable polyvinyl alcohol sponge containing flower-like layered double hydroxide microspheres for efficient removal of As(V) anions and anionic dyes from water. *J. Hazard. Mater.* **367**, 286–292.

Dos Santos, A. J., Cunha, G. D. C., Cruz, D. R. S., Romão, L. P. C. & Martínez-Huitle, C. A. 2019 Iron mining wastes collected from Mariana disaster: reuse and application as catalyst in a heterogeneous electro-Fenton process. *J. Electroanal. Chem.* **848**, 113330.

Dos Santos, A. J., Sirés, I., Alves, A. P. M., Martínez-Huitle, C. A. & Brillas, E. 2020 Vermiculite as heterogeneous catalyst in electrochemical Fenton-based processes: application to the oxidation of Ponceau SS dye. *Chemosphere* **240**, 124838.

Espinoza, C., Romero, J., Villegas, L., Cornejo-Ponce, L. & Salazar, R. 2016 Mineralization of the textile dye acid yellow 42 by solar photoelectro-Fenton in a lab-pilot plant. *J. Hazard. Mater.* **319**, 24–33.

Gao, H. H., Cao, R. Y., Xu, X. T., Xue, J. Y., Zhang, S. W., Hayat, T., Alharbi, N. S. & Li, J. X. 2019 Surface area- and structure-dependent effects of LDH for highly efficient dye removal. *ACS Sustain. Chem. Eng.* **7**, 905–915.

Goncalves, N. P. F., Minella, M., Fabbri, D., Calza, P., Malitesta, C., Mazzotta, E. & Prevot, A. B. 2020 Humic acid coated magnetic particles as highly efficient heterogeneous photo-Fenton materials for wastewater treatments. *Chem. Eng. J.* **390**, 124619.

Govindan, K., Suresh, A. K., Sakthivel, T., Murugesan, K., Mohan, R., Gunasekaran, V. & Jang, A. 2019 Effect of peroxomonosulfate, peroxodisulfate and hydrogen peroxide on graphene oxide photocatalytic performances in methyl orange dye degradation. *Chemosphere* **237**, 124479.

Guan, W. H., Gao, X. C., Ji, G. F., Xing, Y. X., Du, C. F. & Liu, Z. L. 2017 Fabrication of a magnetic nanocomposite photocatalysts Fe_3O_4@ZIF-67 for degradation of dyes in water under visible light irradiation. *J. Solid State Chem.* **255**, 150–156.

Guo, G., Li, X. H., Tian, F., Liu, T. F., Yang, F., Ding, K. Q., Liu, C., Chen, J. S. & Wang, C. Y. 2019 Azo dye decolorization by a halotolerant consortium under microaerophilic conditions. *Chemosphere* **244**, 125510.

Hao, C. Y., Wu, Y., An, Y. J., Cui, B. H., Lin, J. N., Li, X. N., Wang, D. H., Jiang, M. H., Cheng, Z. X. & Hu, S. 2019 Interface-coupling of CoFe-LDH on MXene as high-performance oxygen evolution catalyst. *Materials Today Energy* **12**, 453–462.

Li, J. L., Zhang, S. H., Chen, Y., Liu, T. M., Liu, C. Y., Zhang, X., Yi, M. T., Chu, Z. Y. & Han, X. X. 2017 A novel three-dimensional hierarchical CuAl layered double hydroxide with excellent catalytic activity for degradation of methyl orange. *RSC Adv.* **7**, 29051.

Lin, J., Ye, W., Zeng, H., Yang, H., Shen, J., Darvishmanesh, S., Luis, P., Sotto, A. & Van der Bruggen, B. 2015 Fractionation of direct dyes and salts in aqueous solution using loose nanofiltration membranes. *J. Membr. Sci.* **477**, 183–193.

Liu, J., Liu, A., Wang, W., Li, R. & Zhang, W. 2019 Feasibility of nanoscale zero-valent iron (nZVI) for enhanced biological treatment of organic dyes. *Chemosphere* **237**, 124470.

Luo, X., Liang, C. & Hu, Y. 2019 Comparison of different enhanced coagulation methods for azo dye removal from wastewater. *Sustainability* **11**, 4760.

Ma, K., Cheng, J. P., Zhang, J., Li, M., Liu, F. & Zhang, X. 2016 Dependence of Co/Fe ratios in Co-Fe layered double hydroxides on the structure and capacitive properties. *Electrochim. Acta* **198**, 231–240.

Sanchez, C., Arribart, H. & Guille, M. M. G. 2005 Biomimetism and bioinspiration as tools for the design of innovative materials and systems. *Nat. Mater.* **4**, 277–288.

Sarma, G. K., Khanb, A., El-Tonib, A. M. & Rashida, M. H. 2019 Shape-tunable CuO-$Nd(OH)_3$ nanocomposites with excellent adsorption capacity in organic dye removal and regeneration of spent adsorbent to reduce secondary waste. *J. Hazard. Mater.* **380**, 120838.

Serrà, A., Gómez, E. & Philippe, L. 2019 Bioinspired ZnO-based solar photocatalysts for the efficient decontamination of persistent organic pollutants and hexavalent chromium in wastewater. *Catalysts* **9**, 974.

Velo-Gala, I., Piran-Montaño, J. A., Rivera-Utrilla, J., Sánchez-Polo, M. & Mota, A. J. 2017 Advanced Oxidation Processes based on the use of UVC and simulated solar radiation to remove the antibiotic tinidazole from water. *Chem. Eng. J.* **323**, 605–617.

Wang, C., Gao, J. & Gu, C. 2017 Rapid destruction of tetrabromobisphenol A by iron(III)-tetraamidomacrocyclic ligand/layered double hydroxide composite/H_2O_2 system. *Environ. Sci. Technol.* **51**, 488–496.

Wang, H., Jing, M. M., Wu, Y., Chen, W. L. & Ran, Y. 2018 Effective degradation of phenol via Fenton reaction over CuNiFe layered double hydroxides. *J. Hazard. Mater.* **353**, 53–61.

Wang, Y. J., Song, H. M., Chen, J., Chai, S. N., Shi, L. M., Chen, C. W., Wang, Y. B. & He, C. 2020 A novel solar photo-Fenton system with self-synthesizing H_2O_2: enhanced photo-induced catalytic performances and mechanism insights. *Appl. Surf. Sci.* **512**, 145650.

Xia, D. D., Chen, H. C., Jiang, J. J., Zhang, L., Zhao, Y. D., Guo, D. Q. & Yu, J. W. 2015 Facilely synthesized a phase nickel–cobalt bimetallic hydroxides: tuning the composition for high pseudocapacitance. *Electrochim. Acta* **156**, 108–114.

Xu, Y., Guo, X., Zha, F., Tang, X. & Tian, H. 2020 Efficient photocatalytic removal of orange II by a Mn_3O_4–FeS_2/Fe_2O_3 heterogeneous catalyst. *J. Environ. Manage.* **253**, 109695.

Xue, L., Lü, Z. P., Cheng, Y. Z., Sun, X. Y., Lin, H. T., Xiao, X. L., Li, X. F. & Zhuo, S. P. 2018 Three-dimensional layered double hydroxide membranes: fabrication technique, growth mechanism, and enhanced photocatalytic activity. *Chem. Commun.* **54**, 8494–8497.

Yang, Y. B., Ou, Y. Q., Yang, Y., Wei, X. J., Gao, D., Yang, L., Xiong, Y. L., Dong, H. M., Xiao, P. & Zhang, Y. H. 2019 Modulated transition metal–oxygen covalency in the

octahedral sites of CoFe layered double hydroxides with vanadium doping leading to highly efficient electrocatalysts. *Nanoscale* **11**, 23296.

Yuan, C. Y., Chin, Y. P. & Weavers, L. K. 2018 Photochemical acetochlor degradation induced by hydroxyl radical in Fe-amended wetland waters: impact of pH and dissolved organic matter. *Water Res.* **132**, 52–60.

Zhang, P., Ouyang, S. D., Li, P., Huang, Y. & Ray, L. F. 2019 Enhanced removal of ionic dyes by hierarchical organic three-dimensional layered double hydroxide prepared via soft-template synthesis with mechanism study. *Chem. Eng. J.* **360**, 1137–1149.

Zhao, H., Xia, Q., Xing, H., Chen, D. & Wang, H. 2017 Construction of pillared-layer MOF as efficient visible-light photocatalysts for aqueous Cr(VI) reduction and dye degradation. *ACS Sustain. Chem. Eng.* **5**, 4449–4456.

Zhao, J., Wang, X. R., Chen, F. W., He, C., Wang, X. J., Li, Y. P., Liu, R. H., Chen, X. M., Hao, Y. J., Yang, M. & Li, F. T. 2020 A one-step synthesis of hierarchical porous CoFe-layered double hydroxide nanosheets with optimized composition for enhanced oxygen evolution electrocatalysis. *Inorg. Chem. Front.* **7**, 737–745.

Zong, Y. T., Li, K. T., Tian, R., Lin, Y. J. & Lu, C. 2018 Highly dispersed layered double oxide hollow spheres with sufficient active sites for adsorption of methyl blue. *Nanoscale* **10**, 23191.

First received 31 January 2020; accepted in revised form 4 June 2020. Available online 17 June 2020